12-15-2014

Land Surface Anomalies Preceding the 2010 Russian Heat Wave and a Link to the North Atlantic Oscillation

C. K. Wright
South Dakota State University

K. M. de Beurs
University of Oklahoma

G. M. Henebry
South Dakota State University

Land surface anomalies preceding the 2010 Russian heat wave and a link to the North Atlantic oscillation

2014 Environ. Res. Lett. 9 124015

(http://iopscience.iop.org/1748-9326/9/12/124015)

OPEN ACCESS
IOP Publishing
Environmental Research Letters
Environ. Res. Lett. 9 (2014) 124015 (10pp)
doi:10.1088/1748-9326/9/12/124015

Land surface anomalies preceding the 2010 Russian heat wave and a link to the North Atlantic oscillation

Christopher K Wright[1], Kirsten M de Beurs[2] and Geoffrey M Henebry[1]

[1] Geospatial Sciences Center of Excellence, South Dakota State University, Brookings, SD 57007, USA
[2] Department of Geography and Environmental Sustainability, University of Oklahoma, Norman, OK 73019, USA

E-mail: Christopher.Wright@sdstate.edu

Received 13 June 2014, revised 7 November 2014
Accepted for publication 25 November 2014
Published 15 December 2014

Abstract

The Eurasian wheat belt (EWB) spans a region across Eastern Ukraine, Southern Russia, and Northern Kazakhstan; accounting for nearly 15% of global wheat production. We assessed land surface conditions across the EWB during the early growing season (April–May–June; AMJ) leading up to the 2010 Russian heat wave, and over a longer-term period from 2000 to 2010. A substantial reduction in early season values of the normalized difference vegetation index occurred prior to the Russian heat wave, continuing a decadal decline in early season primary production in the region. In 2010, an anomalously cold winter followed by an abrupt shift to a warmer-than-normal early growing season was consistent with a persistently negative phase of the North Atlantic oscillation (NAO). Regression analyses showed that early season vegetation productivity in the EWB is a function of both the winter (December–January–February; DJF) and AMJ phases of the NAO. Land surface anomalies preceding the heat wave were thus consistent with highly negative values of both the DJF NAO and AMJ NAO in 2010.

Keywords: Russian heat wave, North Atlantic oscillation, land surface, food security, climate change, Arctic amplification, MODIS

1. Introduction

The 2010 Russian heat wave was caused by an unprecedented atmospheric blocking event that persisted from early July to mid-August. Although various aspects of this blocking event have been studied (Dole *et al* 2011, Matsueda 2011, Sedláček *et al* 2011, Lau and Kim 2012, Trenberth and Fasullo 2012), comparatively little attention has been focused on conditions prior to the heat wave; with the exception of Miralles *et al* (2014) who found soil-moisture deficits across most of Southwestern Russia at the heat wave's onset.

In fact, Russia experienced atypical weather for more than six months leading up to the heat wave. First, the winter of 2009/2010 was unusually cold (figure 1); attributable to an anomalously negative phase of the North Atlantic oscillation (NAO, Osborn 2011)—the lowest recorded value in a 60 year NOAA record (figure 2(a)). The severe winter of 2009/2010 was then followed by a warmer-than-normal early growing season. In May of 2010, positive land surface temperature anomalies began to emerge in Russia (figure 1). This temperature reversal coincided with persistence of the anomalously negative NAO through the early season, April–May–June (figure 2(b)). By June, the extent of land surface temperature anomalies South of Moscow was comparable to the height of the heat wave in August (figure 1).

In this study, we examined the unusually warm early season leading up to the Russian heat wave, but not the heat wave itself. Using satellite imagery from the moderate resolution imaging spectroradiometer (MODIS), aboard the AQUA and TERRA satellites, we assessed land surface conditions immediately prior to the heat wave, and over a

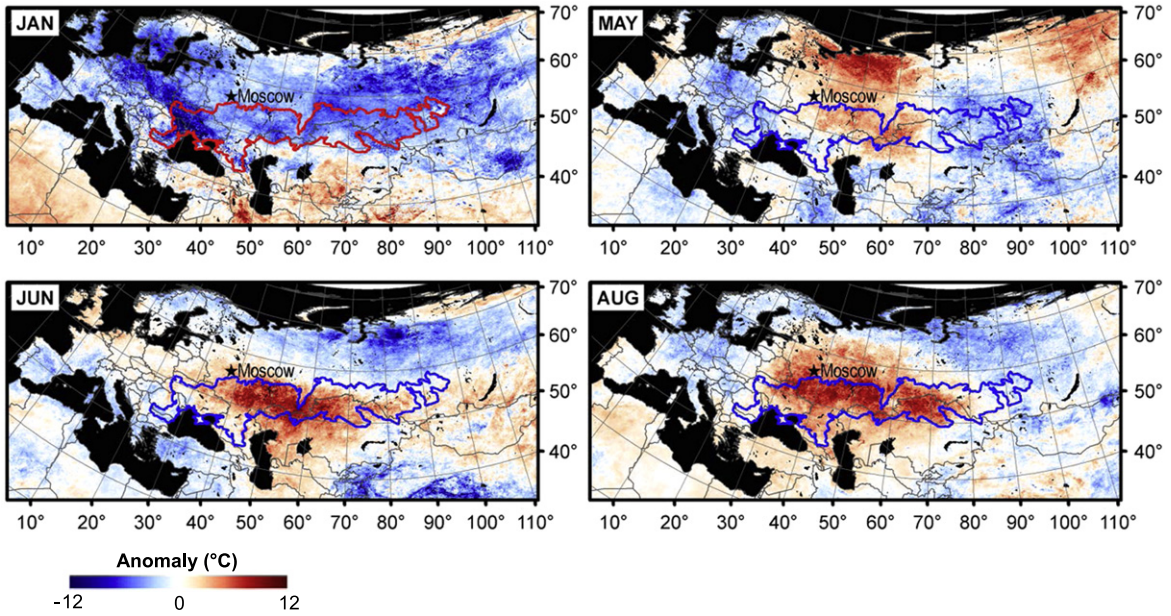

Figure 1. Monthly land surface temperature anomalies during the winter (January) and early season (May, June) preceding the 2010 Russian heat wave and at the height of the heat wave (August). Anomalies are relative to a 2000–2008 baseline (NASA 2010a). Red and blue outlines indicate extent of the Eurasian wheat belt (EWB).

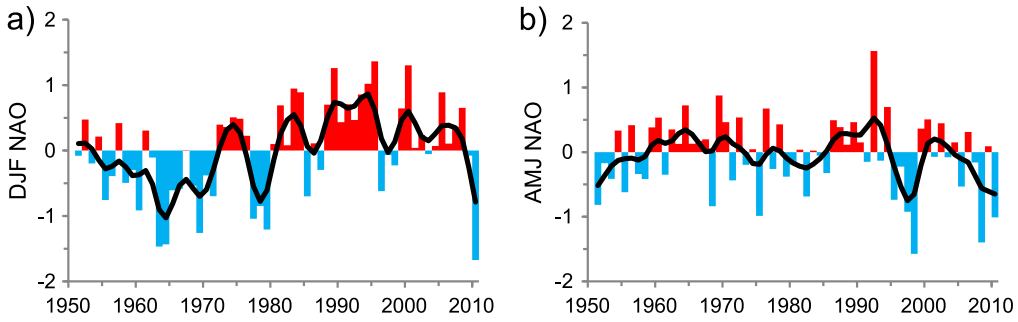

Figure 2. Seasonally-averaged values of the North Atlantic oscillation (NAO) for the period 1951–2010. (a) The winter NAO (December–February; DJF). (b) The early season NAO (April–June; AMJ). Seasonal averages calculated from monthly NAO values (NOAA CPC 2011). Black lines are smoothed values using a 10 year Gaussian-weighted filter.

longer term period from 2000 to 2010. To explain land surface anomalies preceding the Russian heat wave, and longer-term regional trends, we focused on statistical teleconnections involving both winter and early season phases of the NAO.

Our study area encompassed a region we term the Eurasian wheat belt (EWB; see outline in figure 1). The EWB accounts for nearly 15% of global wheat production (US Department of Agriculture (USDA) Foreign Agricultural Service 2010) and is projected to make an increasing contribution to global food security (Fischer *et al* 2005, World Bank 2009, Lioubimtseva and Henebry 2012). However, climate change has contributed to an estimated 3–5-fold increase in the probability of heat waves as severe as the 2010 event (Rahmstorf and Coumou 2011, Otto *et al* 2012). Compared globally; Lobell *et al* (2011) found that reductions in agricultural productivity attributable to global warming were most severe in Russia. It is thus critically important to identify those broad-scale atmospheric processes that influence the EWB's climatic vulnerability.

2. Materials and methods

2.1. Study area

The EWB spans an arc of fertile soils across Southern Russian, Northern Kazakhstan, and nearly all of Ukraine. We delineated boundaries of the EWB using the United Nations Food and Agricultural Organization World Soil Map (United Nations Food and Agriculture Organization (FAO) 2003). The Western and central portions of the EWB coincide with the 'Black-Earth Region' North of the Black Sea, where dark-colored mollisols (Chernozems) are well-suited to small-grain cultivation. The Eastern EWB is characterized by related mollisols—Kastanozems and Phaeozems. We defined the Northern boundary of the EWB based on transitional soils (Greyzems and Luvisols) occupying the ecotone between steppe to the South and temperate forest to the North (United Nations Food and Agriculture Organization (FAO) 2003).

2.2. Data

We assessed vegetation productivity using a remotely-sensed index sensitive to vegetated landscapes, the normalized difference vegetation index (NDVI). The NDVI exploits differences in spectral reflectance characteristic of green vegetation, i.e., low reflectance in the visible red wavelength (RED) and high reflectance in the near-infrared (NIR), and is calculated as: NDVI = (NIR – RED)/(NIR + RED). We calculated NDVI from MODIS imagery at 500 m spatial resolution using the nadir bi-directional reflectance distribution function adjusted reflectance (NBAR) product (NASA 2010b). MODIS-NBAR data is standardized to a nadir (vertical) viewing angle which for purposes of temporal analysis reduces noise associated with non-constant instrument view angle and atmospheric effects. It is distributed as 16 day rolling composites updated every eight days. To span the early growing season in the EWB, we used ten NDVI composites from mid-April to the last week in June.

Monthly values of the NAO index were obtained from the NOAA Climate Prediction Center (NOAA Climate Prediction Center 2011). This version of the NAO index is generated by rotated principal components analysis (Barnston and Livezey 1987). Empirical relationships between the NAO and surface air temperature were analyzed over the period 1951–2010 using seasonally-averaged surface (2 m) air temperature data from the NCEP/NCAR Reanalysis v1 (Kalnay *et al* 1996). A similar analysis with respect to precipitation was conducted using monthly precipitation data from the Global Precipitation Climatology Centre (GPCC) Reanalysis v5 (Rudolf *et al* 2010). In this case, GPCC data were not available for 2010. Plant water availability in the EWB was assessed using monthly values of the self-calibrated Palmer drought severity index (scPDSI) obtained from the NOAA Earth System Research Laboratory (NOAA Earth System Research Laboratory 2011, Dai 2011).

2.3. Mann–Kendall (MK) trend analysis

Geospatially referenced NDVI time series were analyzed using the MK trend test on values averaged over the early growing season. The MK trend test is a nonparametric method well-suited for identifying monotonic trends in time series that contain missing values and/or do not meet normality assumptions (Hirsch and Slack 1984). In this case, the MK test was used to assess the presence of monotonic trends over the period 2000–2010. Note that we did not estimate rates of change and make no inferences outside that period. Rather, our objective was to identify locations (500 m pixels) exhibiting directional change from 2000 to 2010 that was statistically distinguishable from random variation.

3. Results

The NDVI is positively correlated with the amount of photosynthetic biomass per unit area (green leaf area) and thus is an effective proxy for plant primary production (Tucker and Sellers 1986), especially in semi-arid settings like the EWB where leaf area and NDVI are strongly correlated (Fan *et al* 2009, Li and Guo 2012). As such, we use the terms 'NDVI' and 'primary production' synonymously. Where the unit of analysis is the NDVI, an interpretation of results is often best expressed in terms of plant primary production underlying the NDVI.

With respect to broad vegetation provinces, the EWB occupies a semi-arid transitional zone between forest and taiga to the North and the Caspian and Kazakh deserts to the South (Olson *et al* 2001). This transitional zone, consisting mainly of steppe and forest steppe, is reflected in a North–South declining gradient in mean early season NDVI (primary production) for our baseline period, 2000–2009 (figure 3(a)). A similar declining gradient is found from West to East across the region.

Comparison of mean early season NDVI in 2010 with the 2000–2009 baseline shows that substantial reductions in early season primary production occurred prior to the Russian heat wave (figure 3(b)). Negative land surface anomalies spanned nearly the entire EWB from central Ukraine Eastward, with highly negative anomalies concentrated in Northern Kazakhstan. Positive NDVI anomalies were concentrated in the far Western and Southwestern EWB (figure 3(b)).

Land surface anomalies in 2010 marked the continuation of a longer-term decline in early season primary production in the EWB. From 2000 to 2010, regionally-averaged NDVI dropped more than 12% (figure 4(a)). This decline coincided with a comparable drop in regionally-averaged values of the self-calibrated Palmer drought severity index (scPDSI). However, note that mean scPDSI increased slightly in 2010. In this case, regional averaging included higher scPDSI values in the Western EWB in 2010. Similarly, the modest drop in regionally-averaged NDVI from 2009 to 2010 reflects positive NDVI anomalies in the Western EWB (figure 3(b)). In contrast with regional drying during the 2000 s, the longer-term scPDSI time series from 1951 to 2010 has no overall trend (figure 4(b)); suggesting that recent drought and its effects on regional primary productiopm may simply represent normal multi-decadal variability.

We also assessed NDVI trends from 2000 to 2010 on a spatially-explicit basis. Statistically significant ($p < 0.05$) declines in early season primary production occurred across most of the region (figure 3(c)) with a spatial pattern closely resembling 2010 anomalies (figure 3(b)). Only in the far Western EWB were trends significantly positive (figure 3(c)).

Next, we considered whether the NAO could have played a role in the cold winter/warm early season pattern observed in 2010 (figure 1). The winter NAO has a well-documented effect on surface air temperatures across Western Eurasia through its influence on the Atlantic storm track and warm air advection from the North Atlantic into Northern Europe (Hurrell 1995). Figure 5(a) shows that in the EWB, positive NAOs are associated with warmer winters, negative NAOs with colder winters. This teleconnection is reversed during the early season (figure 5(b)). Thus, negative (positive) NAOs are associated with warmer (cooler) AMJ temperatures in the EWB—consistent with a flip in temperature regime when the

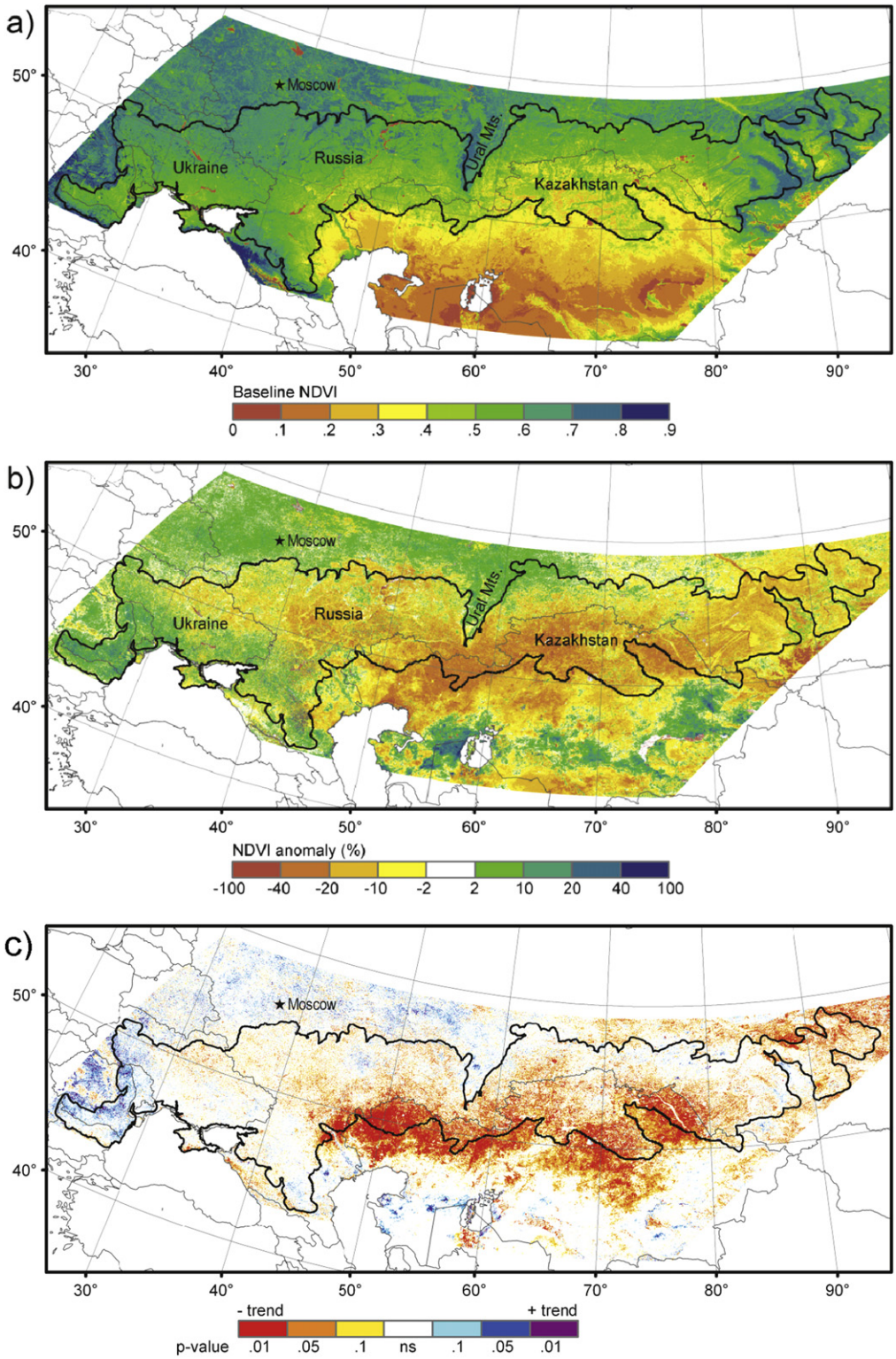

Figure 3. (a) Mean early season NDVI for the period 2000–2009. Early season NDVI is averaged over ten MODIS composites from mid-April to the end of June in each year. (b) Early season NDVI anomalies in 2010 relative to the 2000–2009 baseline. (c) Mann–Kendall analysis of trends in mean early season NDVI for the period 2000–2010. The Eurasian wheat belt is indicated by black outline. Spatial resolution is 500 m.

NAO is persistently negative from winter through the early season.

During the winter NAO's negative phase, the Atlantic storm track shifts Southward (Hurrell 1995). This influence extends into the Western EWB, where negative NAOs are associated with increased DJF precipitation, positive NAOs with drier winters (figure 6(a)). This teleconnection is thus consistent with the positive precipitation anomalies observed

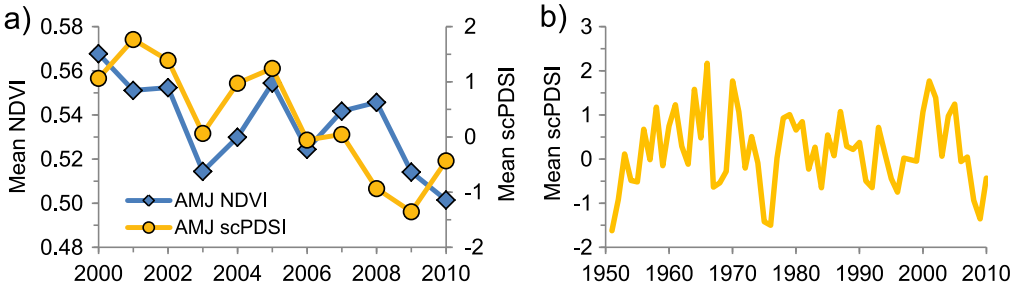

Figure 4. (a) Regionally-averaged time series of early season NDVI and early season self-calibrated Palmer drought severity index (scPDSI). In each year, early season NDVI was averaged across the EWB over the 10 MODIS composites from mid-April to the end of June. Early season scPDSI was averaged regionally from monthly scPDSI values for the months of April–May–June. (b) Regionally-averaged scPDSI times series from 1951 to 2010. By Mann–Kendall trend test, this time series has no overall trend ($p = 0.342$).

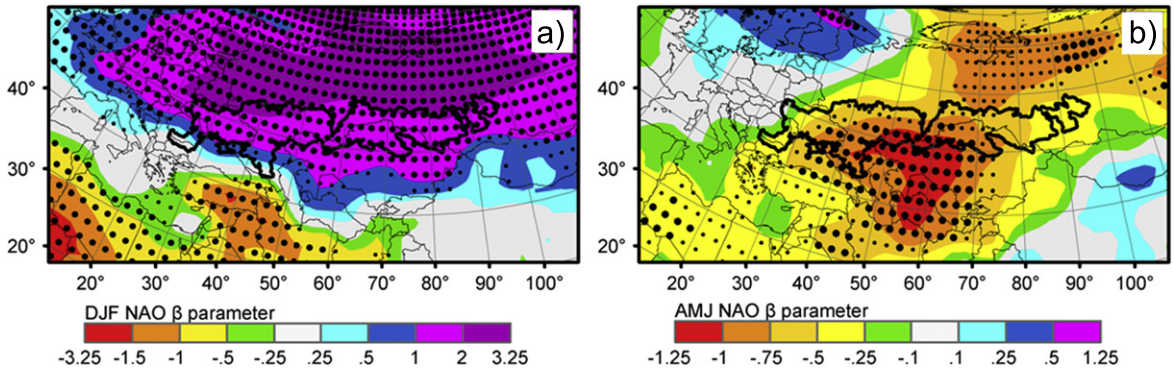

Figure 5. (a) Slope (β) of linear regressions between the DJF NAO and mean DJF surface air temperature (2 m) for the period 1951–2010 using monthly average surface air temperature data from the NCEP/NCAR Reanalysis v1 (Kalnay *et al* 1996). Larger circles indicate highly significant regressions at the $p < 0.01$ level; smaller circles indicate significance at the $p < 0.05$ level. Results at 2.5° spatial resolution smoothed for display by bilinear interpolation. (b) As in (a), but for the AMJ NAO and mean AMJ surface air temperature.

in DJF 2010 (figure 6(b)). During the early season, figure 6(c) shows that in central portions of the EWB, negative (positive) NAOs are associated with decreased (increased) AMJ precipitation. While this teleconnection is mostly consistent with negative precipitation anomalies in AMJ 2010, it does not explain negative anomalies West of approximately 50°E longitude (figure 6(d)).

Lastly, we focused on the NAO as a driver of early season primary production in the EWB. Here we used multivariate linear regression with the DJF and AMJ phases of the NAO as independent variables and mean early season NDVI as the response (figure 7). This model structure was justified by an absence of correlation between the DJF and AMJ NAO over the 60 year NOAA record ($r = 0.08$, $p = 0.57$; figure 2).

Slope coefficients for the DJF NAO were predominately positive across the region (figure 7(a)). In the EWB, negative DJF NAOs are associated with reduced primary production during the early season, positive DJF NAOs with increased productivity. This pattern likely reflects a lagged, negative effect of colder winters when the DJF NAO is negative versus a positive effect of warmer winters during positive NAOs (e.g., figure 5(a)).

Slopes coefficients for the AMJ NAO were less uniform across the region. In the Western and Northern EWB, slope values were primarily negative (figure 7(b)). These are the more mesic portions of the EWB, as illustrated by regional productivity gradients (figure 3(a)), where primary production is likely more limited by early season air temperatures than moisture availability. Thus, given the AMJ temperature teleconnection (figure 5(b)), a positive (negative) effect of warmer (cooler) air temperatures is expected when the AMJ NAO is negative (positive). By contrast, across much of the Southern and Eastern two-thirds of the EWB, slope coefficients were generally positive (figure 7(b)); indicating an opposite effect of the AMJ NAO. Here, in the more arid portions of the EWB (figure 3(a)), negative NAOs are associated with reduced AMJ primary production, positive NAOs with increased productivity. This relationship likely reflects the influence of AMJ precipitation and temperature teleconnections (figures 5(b) and 6(c)) with respect to drought, e.g., dry, warmer-than-normal early seasons during negative NAOs. This is not to say that warmer air temperatures are not expected to positively affect primary production during the initial phase of plant growth when spring soil-moisture is likely adequate. However, note that peak NDVI (leaf area) in the EWB typically occurs in mid-June (result not shown); indicating that the AMJ period encompasses a substantial proportion (if not the majority) of primary production over the entire growing season. Integrated over these three months, we expect vegetation in the Southern EWB to be more water-limited than temperature-limited; with warmer-than-normal

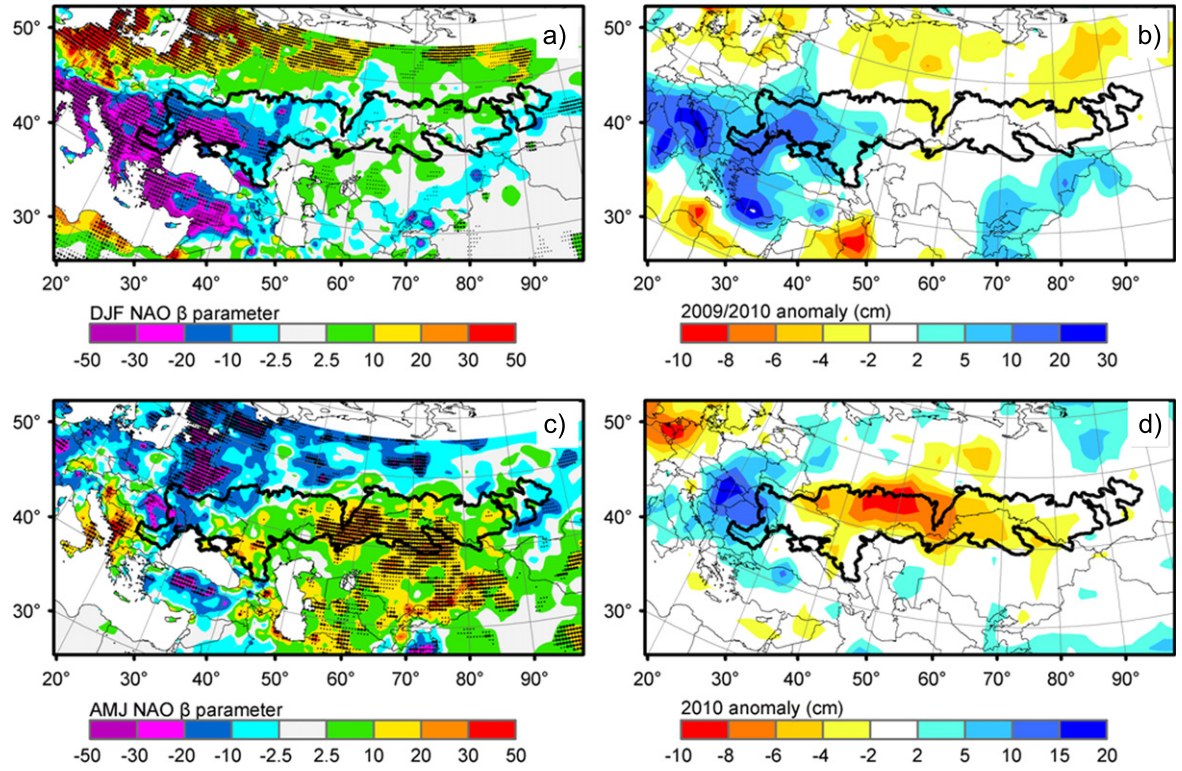

Figure 6. (a) Slope (β) of linear regressions between the DJF NAO and DJF precipitation for the period 1951–2009 using monthly precipitation data from GPCC Reanalysis v5 (Rudolf *et al* 2010). Results at 0.5° spatial resolution smoothed for display by bilinear interpolation. Larger (more dense) circles indicate regressions statistically significant at the $p < 0.01$ level. Smaller (less dense) circles indicate significance at the $p < 0.05$ level. (b) 2010 DJF precipitation anomalies from the NCEP-CAMS (Ropelewski *et al* 1984). Results at 2.5° spatial resolution smoothed by bilinear interpolation. (c) As in (a), but for the AMJ NAO and AMJ precipitation. (d) As in (b), but for 2010 AMJ precipitation anomalies.

air temperatures during negative NAOs likely exacerbating plant moisture-stress.

To summarize, within those parts of the EWB exhibiting both declining primary production from 2000 to 2010 (figure 3(c)) and highly negative land surface anomalies in 2010 (figure 3(b)), the combined influence of the DJF and AMJ phases of the NAO is reflected in coefficients of determination generally exceeding 50% (figure 7(c)).

4. Discussion

We found land surface anomalies preceding the Russian heat wave that were empirically consistent with a persistently negative NAO in 2010. Given that the NDVI is an effective proxy for leaf area in semi-arid ecosystems (Fan *et al* 2009, Li and Guo 2012), these anomalies point to the importance of an accurate representation of leaf area dynamics (vegetation phenology) before and during the Russian heat wave, as has been recently shown in simulations of the 2003 European heat wave (Stéfanon *et al* 2012a). Notably, reductions in early season NDVI prior to the European heat wave were also concentrated in agricultural landscapes (Zaitchik *et al* 2006).

Miralles *et al* (2014) recently demonstrated the importance of soil drying and resulting increases in sensible heat flux as drivers of air temperature extremes during the Russian heat wave. Interestingly, they found soil moisture anomalies at the heat wave's onset closely resembling the pattern of land surface anomalies that we document. Areas with initial soil moisture deficits later exhibited the highest absolute temperatures recorded during the heat wave. However, Miralles *et al* (2014) also found that such deficits were not a necessary pre-condition for an event as spatially extensive as the Russian heat wave. In areas where soil moisture deficits were not initially present, atmospheric blocking effects including warm air advection and high insolation under clear skies were sufficiently strong enough to force land-atmosphere feedbacks that rapidly dried soils, tipped the surface energy balance toward high sensible heat fluxes, and entrained hot air within the atmospheric boundary layer (Miralles *et al* 2014). In light of these results, land surface anomalies linked to the NAO might be best treated as playing a contributing role in the Russian heat wave, in that they affected the partitioning of latent and sensible heat at the heat wave's onset, but not a causal one, such that an anomalously negative NAO was not a necessary pre-condition. Similarly, Stéfanon *et al* (2012b) found that a characteristically Russian-type of heat wave is dominated by synoptic circulation, not spring drought. On the other hand, land surface pre-conditioning has been shown to increase the sensitivity of summer temperatures in Europe (daily maximum air temperature) to atmospheric blocking (Fischer *et al* 2007, Hirschi *et al* 2011, Quesada *et al* 2012).

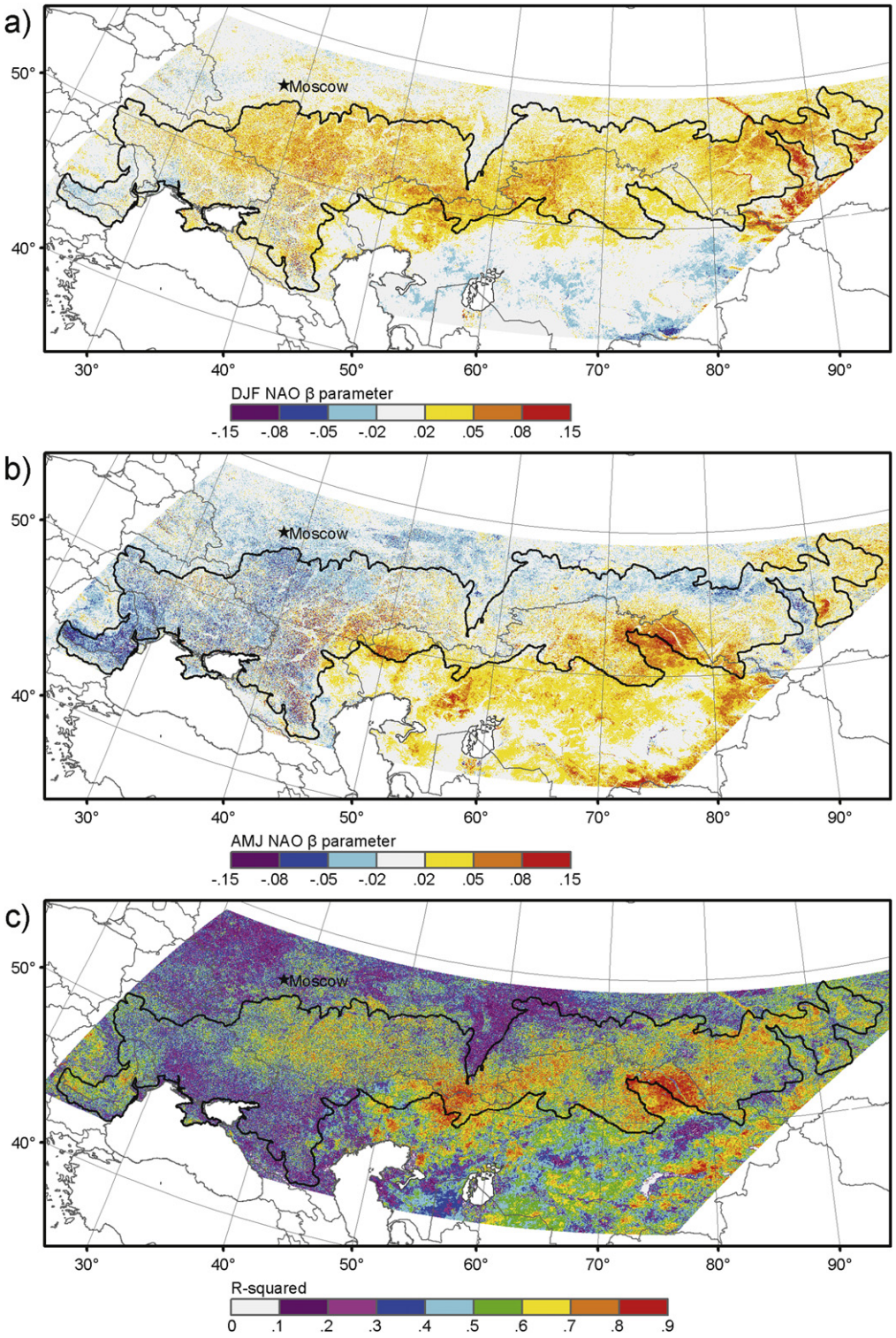

Figure 7. Linear regression of mean early season NDVI against the DJF and AMJ phases of the NAO for the period 2000–2010. (a) Slope coefficients corresponding to the DJF NAO. (b) Slope coefficients corresponding to the AMJ NAO. (c) Coefficients of determination for regressions. Spatial resolution is 500 m.

We expect that coupled atmosphere-land surface models taking into account both leaf area *and* soil-moisture anomalies prior to the Russian heat wave will better resolve the relative importance of synoptic circulation versus land surface preconditioning in 2010.

The linkage between a negative AMJ NAO and reduced primary production in the EWB (figure 7(b)) is consistent with teleconnections related to drought, i.e., with AMJ surface air temperature (figure 5(b)) and precipitation (figure 6(c)). However, the nearly uniform influence of the

winter NAO on the EWB (figure 7(a)) is not as intuitive. Previous studies have shown a similarly-lagged statistical relationship between the winter NAO and early season NDVI in central Eurasia (Wang and You 2004, de Beurs and Henebry 2008); with evidence that negative winter NAOs are associated with a delayed start of season (SOS), positive winter NAOs with an early SOS. However, we found no evidence of a delayed SOS in 2010, or a trend in SOS during the 2000 s (result not shown). In fact, there was an early snowmelt prior to the Russian heat wave (Barriopedro *et al* 2011). An alternate explanation could be the winter NAO's effect on overwintering survival of winter wheat. In 2010, winterkill totaling nearly two-million hectares of wheat was reported in Western Russia (Vocke *et al* 2010). However, we suspect that negative winter NAOs impact early season plant growth via deep soil freezing during anomalously cold winters; with subsequent effects on moisture availability in spring. In Southern Russia, Cherenkova (2012) reported reduced infiltration of snowmelt in spring 2010 due to an unusually deep layer of frozen soil. In addition, so-called 'physiological drought' can occur when plant roots restricted to the upper soil profile by frozen sub-soils quickly exhaust available soil moisture (Repo *et al* 2008). In sum, there is a clear need for further study to explain the winter NAO's lagged influence in the EWB.

Empirical relationships found here point to the need for mechanistic studies of atmospheric circulation into the EWB during the months of April–May–June (AMJ); a 'shoulder season' not typically considered. For example, the AMJ temperature pattern in figure 5(b) is indicative of Northward advection of warm air from North Africa and the Middle East during a negative NAO; suggesting the likely importance of regional blocking patterns during the early season. To the best of our knowledge, this teleconnection has not been previously described. Such an absence is notable given the AMJ pattern's pronounced contrast with effects of the winter NAO (figure 5(a)), where advection from the North Atlantic plays a primary role (Hurrell 1995). Studies of the NAO's influence on the East Asian summer monsoon have shown that an anomalously negative spring NAO can induce persistent sea surface temperature anomalies in the North Atlantic; exciting a Rossby wave train across Eurasia during *summer* and enhancing atmospheric blocking centered on the Ural Mountains (Wu *et al* 2009, 2012). Whether Rossby wave propagation during the early season might also explain the AMJ temperature teleconnection is an important question.

Declining primary production in the EWB (figure 3(c)) was consistent with a decadal decline in both the DJF and AMJ phases of the NAO (figure 2). Such trends during the 2000 s may simply reflect normal multi-decadal variability (e.g., figure 4(b)). However, a number of studies have now shown that reduced sea ice extent in the Arctic can induce wintertime circulation anomalies resembling a negative NAO (Francis *et al* 2009, 2012, Honda *et al* 2009, Seierstad and Bader 2009, Overland *et al* 2011, Jaiser *et al* 2012, Liu *et al* 2012, Screen *et al* 2013, Tang *et al* 2014). This raises the possibility that a negative shift in mean Arctic ice extent due to anthropogenic forcing (Comiso 2006, Serreze *et al* 2007, Wang and Overland 2009) could shift the probability distribution of the winter NAO toward its negative phase (Strong and Magnusdottir 2009, Jaiser *et al* 2012). Given our results, such a shift could pose a previously unrecognized climate-change risk to wheat production in the EWB. We note, however, that comprehensive GCM studies do not produce an unequivocal, negative forcing of the winter NAO in response to projected sea ice losses (Deser *et al* 2010, Gillett and Fyfe 2013).

Potential negative forcing of the NAO during the AMJ shoulder season has not been investigated. However, others have proposed a link between rapid Arctic climate change (Arctic amplification) and an increase in Rossby wave amplitudes (Francis and Vavrus 2012, Petoukhov *et al* 2014, Tang *et al* 2014), i.e., a more meandering atmospheric circulation roughly analogous to a negative NAO. This theory is controversial (Barnes 2013, Screen and Simmonds 2013a, 2013b), but we draw attention to it here because of the EWB's apparent sensitivity to the NAO's negative phase. If Arctic amplification does indeed effect a more meandering circulation at mid-latitudes, the EWB may prove to be an early responder to such a shift.

In sum, our results and those of others (Lobell *et al* 2011, Rahmstorf and Coumou 2011, Otto *et al* 2012) clearly show that the wheat growing regions of Russia, Ukraine, and Kazakhstan form a nexus of unusual environmental change. Given projections of an increasing contribution to global food security by the EWB (Fischer *et al* 2005, World Bank 2009, Lioubimtseva and Henebry 2012), we recommend the region as an important focal area for future climate change studies—emphasizing the EWB's potential vulnerability to Arctic amplification.

References

Barnes E A 2013 Revisiting the evidence linking Arctic amplification to extreme weather in midlatitudes *Geophys. Res. Lett.* **40** 4734–9

Barnston A G and Livezey R E 1987 Classification, seasonality and persistence of low-frequency atmospheric circulation patterns *Mon. Weather Rev.* **115** 1083–126

Barriopedro D, Fischer E M, Luterbacher J, Trigo R M and Garcia-Herrea R 2011 The hot summer of 2010: redrawing the temperature record map of Europe *Science* **332** 220–4

Cherenkova E A 2012 Analysis of extensive atmospheric droughts features in the South of European Russia *Arid Ecosystem* **2** 209–15

Comiso J 2006 Abrupt decline in the Arctic winter sea ice cover *Geophys. Res. Lett.* **33** L027341

Dai A 2011 Characteristics and trends in various forms of the palmer drought severity index during 1900–2008 *J. Geophys. Res.* **116** D12115

de Beurs K M and Henebry G M 2008 Northern annular mode effects on the land surface phenologies of Northern Eurasia *J. Clim.* **21** 4257–79

Deser C, Tomas R, Alexander M and Lawrence D 2010 The seasonal atmospheric response to projected Arctic sea ice loss in the late 21st century *J. Clim.* **23** 333–50

Dole R *et al* 2011 Was there a basis for anticipating the 2010 Russian heat wave? *Geophys. Res. Lett.* **38** L06702

Fan L, Gao Y, Brück H and Bernhofer C 2009 Investigating the relationship between NDVI and LAI in semi-arid grassland in inner Mongolia using *in situ* measurements *Theor. Appl. Climatol.* **95** 151–6

Fischer E M, Seneviratne S I, Luthi D and Schar C 2007 Contribution of land-atmosphere coupling to recent European summer heat waves *Geophys. Res. Lett.* **34** L06707

Fischer G M, Shah M, Tubiello F and Van Velhuizen H 2005 Socio-economic and climate change impacts on agriculture: an integrated assessment 1990–2080 *Phil. Trans. R. Soc.* B **360** 2067–83

Francis J A, Chan W, Leathers D, Miller J and Veron D 2009 Winter Northern Hemisphere weather patterns remember summer Arctic sea-ice extent *Geophys. Res. Lett.* **36** L07503

Francis J A and Vavrus S J 2012 Evidence linking Arctic amplification to extreme weather in mid-latitudes *Geophys. Res. Lett.* **39** L06801

Gillett N P and Fyfe J C 2013 Annular mode changes in the CMIP5 simulations *Geophys. Res. Lett.* **40** 1189–93

Hirsch R M and Slack J R 1984 A nonparametric trend test for seasonal data with serial dependence *Water Resour. Res.* **20** 727–32

Hirschi M *et al* 2011 Observational evidence for soil-moisture impact on hot extremes in Southeastern Europe *Nat. Geosci.* **4** 17–21

Honda M, Inoue J and Yamane S 2009 Influence of low Arctic sea-ice minima on anomalously cold Eurasian winters *Geophys. Res. Lett.* **36** L00870

Hurrell J W 1995 Decadal trends in the North Atlantic Oscillation: regional temperatures and precipitation *Science* **269** 676–9

Jaiser R, Dethloff K, Handorf D, Rinke A and Cohen J 2012 Impact of sea ice cover changes on the Northern Hemisphere atmospheric winter circulation *Tellus* A **64** 1–11

Kalnay E *et al* 1996 The NCEP/NCAR Reanalysis 40 year Project *Bull. Am. Meteorol. Soc.* **77** 437–71

Lau K M and Kim K-M 2012 The 2010 Pakistan flood and Russian heat wave: teleconnection of hydrometeorological extremes *J. Hydrometeorology* **13** 392–403

Li Z and Guo X 2012 A suitable NDVI product for monitoring spatiotemporal variations of LAI in semiarid mixed grassland *Can. J. Remote Sens.* **38** 683–94

Liu J, Curry J A, Wang H, Song M and Horton R M 2012 Impact of declining Arctic sea ice on winter snowfall *Proc. Natl Acad. Sci. USA* **109** 4074–9

Lioubimtseva E and Henebry G M 2012 Grain production trends in Russia, Ukraine and Kazakhstan: new opportunities in increasingly unstable world? *Frontiers Earth Sci.* **6** 157–66

Lobell D B, Schlenker W and Costa-Roberts J 2011 Climate trends and global crop production since 1980 *Science* **333** 616–20

Matsueda M 2011 Predictability of Euro-Russian blocking in summer of 2010 *Geophys. Res. Lett.* **3** L06801

Mirralles D G, Teuling A J, van Heerwaarden C C and de Arellano J V-G 2014 Mega-heatwave temperatures due to combined soil desiccation and atmospheric heat accumulation *Nat. Geosci.* **7** 345–9

NASA 2010a Average land surface temperature (http://neo.sci.gsfc.nasa.gov/view.php?datasetId=MOD_LSTD_CLIM_M)

NASA 2010b Nadir BRDF-adjusted reflectance 16-day L3 global 500 m (https://lpdaac.usgs.gov/products/modis_products_table/mcd43a4)

NOAA Climate Prediction Center 2011 Standardized Northern hemisphere teleconnection Indices (ftp://ftp.cpc.ncep.noaa.gov/wd52dg/data/indices/tele_oldindex.nh)

NOAA Earth System Research Laboratory 2011 Palmer Drought Severity Index (PDSI) from NCAR (www.esrl.noaa.gov/psd/data/gridded/data.pdsi.html)

Olson D M *et al* 2001 Terrestrial ecoregions of the world: a new map of life on Earth *Bioscience* **51** 933–8

Otto F E L, Massey N, van Oldenborgh G J, Jones R G and Allen M R 2012 Reconciling two approaches to attribution of the 2010 Russian heat wave *Geophys. Res. Lett.* **39** L04702

Osborn T J 2011 Winter 2009/2010 temperatures and a record-breaking North Atlantic Oscillation index *Weather* **66** 19–21

Overland J E, Wood K R and Wang M 2011 Warm Arctic-cold continents: climate impacts of the newly open Arctic Sea *Polar Res.* **30** 15787

Petoukhov V, Rahmstorf S, Petri S and Schellnhuber H J 2014 Quasiresonant amplification of planetary waves and recent Northern Hemisphere weather extremes *Proc. Natl Acad. Sci. USA* doi:10.1073/pnas.1222000110

Quesada B, Vautard R, Yiou P, Hirschi M and Seneviratne S 2012 Asymmetric European summer heat predictability from wet and dry southern winters and springs *Nat. Clim. Change* **2** 736–741

Rahmstorf S and Coumou D 2011 Increase of extreme events in a warming world *Proc. Natl Acad. Sci. USA* **108** 17905–9

Repo T, Lehto T and Finér L 2008 Delayed soil thawing affects root and shoot functioning and growth in Scots pine *Tree Physiol.* **28** 1583–91

Ropelewski C F, Janowiak J E and Halpert M S 1984 *The Climate Anomaly Monitoring System (CAMS)* (Washington DC: Climate Analysis Center, NWS, NOAA)

Rudolf B, Becker A, Schneider U, Meyer-Christoffer A and Ziese M 2010 *GPCC Status Report December 2010* (Offenbach, Germany: Global Precipitation Climatology Centre)

Screen J A, Deser C, Simmonds I and Tomas R 2013 The atmospheric response to three decades of observed Arctic sea ice loss *J. Clim.* **26** 1230–48

Screen J A and Simmonds I 2013a Exploring links between Arctic amplification and mid-latitude weather *Geophys. Res. Lett.* **40** 959–64

Screen J A and Simmonds I 2013b Caution needed when linking weather extremes to amplified planetary waves *Proc. Natl Acad. Sci. USA* doi:10.1073/pnas.1304867110

Sedláček J, Martius O and Knutti R 2011 Influence of subtropical and polar sea-surface temperature anomalies on temperatures in Eurasia *Geophys. Res. Lett.* **38** L12803

Seierstad I A and Bader J 2009 Impact of a projected future Arctic Sea ice reduction on extratropical storminess and the NAO *Clim. Dyn.* **33** 937–43

Serreze M C, Holland M M and Stroeve J 2007 Perspectives on the Arctic's shrinking sea-ice cover *Science* **315** 1533–6

Stéfanon M, Drobinski P, D'Andrea F and de Noblet-Ducoudré N 2012a Effects of interactive vegetation phenology on the 2003 summer heat waves *J. Geophys. Res.* **117** D24103

Stéfanon M, D'Andrea F and Drobinski P 2012b Heatwave classification over Europe and the Mediterranean region *Environ. Res. Lett.* **7** 014023

Strong C and Magnusdottir G 2009 Observed feedback between winter sea ice and the North Atlantic oscillation *J. Clim.* **22** 6021–32

Tang Q, Zhang X and Francis J A 2014 Extreme summer weather in Northern mid-latitudes linked to a vanishing cryosphere *Nat. Clim. Change* **4** 45–50

Trenberth K E and Fasullo J T 2012 Climate extremes and climate change: The Russian heat wave and other climate extremes of 2010 *J. Geophys. Res.* **117** D17103

Tucker C and Sellers P 1986 Satellite remote sensing of primary production *Int. J. Remote Sens.* **7** 1395–416

US Department of Agriculture (USDA) Foreign Agricultural Service 2010 Grain: World Markets and Trade (*Circular Series FG 10-10*) (Washington, DC: USDA)

United Nations Food and Agriculture Organization (FAO) 2003 The digitized soil map of the world and derived soil properties *FAO Land and Water Digital Media Series No. 1*

Vocke G, Allen E and Liefert O 2010 *Wheat outlook: WHS-10e* (Washington, DC: Economic Research Service, USDA)

Wang G and You L 2004 Delayed impact of the North Atlantic oscillation on biosphere productivity in Asia *Geophys. Res. Lett.* **31** L12210

Wang M and Overland J E 2009 A sea ice free summer Arctic within 30 years? *Geophys. Res. Lett.* **36** L07502

Wu Z, Wang B, Li J and Jin F-F 2009 An empirical seasonal prediction model of the East Asian summer monsoon using ENSO and NAO *J. Geophys. Res.* **114** D18120

Wu Z, Li J, Jiang Z, He J and Zhu X 2012 Possible effects of the North Atlantic oscillation on the strengthening relationship between the East Asian summer monsoon and ENSO *Int. J. Climatol.* **32** 794–800

World Bank 2009 *Adapting to Climate Change in Europe and Central Asia* (Washington, DC: World Bank) (www.worldbank.org/eca/climate/ECA_CCA_Full_Report.pdf)

Zaitchik B F, Macalady A K, Bonneau L R and Smith R B 2006 Europe's 2003 heat wave: a satellite view of impacts and land–atmosphere feedbacks *Int. J. Clim.* **26** 743–69